

Appendix A Optimization of PCNBC planar design and device fabrication

The cavity loss of PCNBC is minimized by achieving a Gaussian-like field attenuation profile in the symmetrical planar design^[1] in Figure S1. The filling factor, which is defined as the ratio between hole radius and hole period, is quadratically decreased from 0.32 to 0.25 in the tapered region and fixed in the mirror region. Constant hole period a and the number of mirror segments m are set to 330 nm and 16 respectively. The specialized design contributes to the strengthen of light-matter interactions and minification of the device.

The PCNBC, together with silicon waveguide (600 nm in width) and a pair of grating couplers, is defined by electron beam lithography (EBL) and then inductively coupled plasma (ICP) etching. Ferroelectric dielectric P(VDF-TrFE) with 300 nm thickness was realized by sol-gel spin-coating method. It also acts as a cladding for Si waveguide to avoid strong absorption of light by metal electrodes. Then, the patterned metal as the top electrode of the ferroelectric capacitor was fabricated above PCNBC and ferroelectric dielectric.

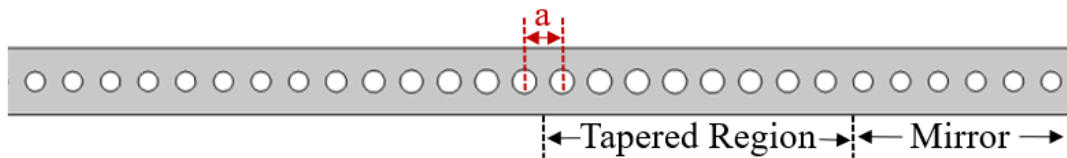


Figure S1. The symmetrical planar design of PCNBC.

Appendix B Transmission spectrum measurement of fabricated device

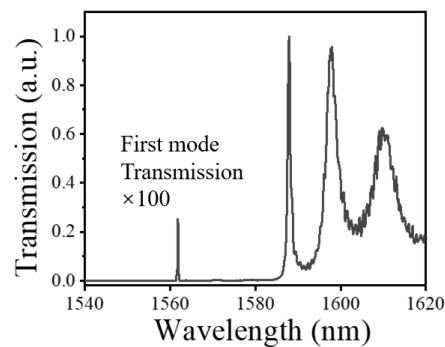


Figure S2. Measured transmission spectrum of PCNBC, transmission of the first mode is magnified.

The signal light transmitting into the grating couplers is generated by Yenista T100S-HP/CL with polarization controlled by fiber polarization controller (FPC). Scanning result is shown in Figure S2. The resonant wavelength of PCNBC's first mode appears at 1562.33 nm.

After the successive deposition of P(VDF-TrFE) film and Au electrode, significant red shifts of 17.3 nm and 5.79 nm are observed respectively, as presented in Figure S3. It's concluded that the replacement of air cladding by P(VDF-TrFE) film and further metal layer changes the refractive index in the PCNBC region. Also, the quality factor undergoes a sharp decline from 20290 and 20250 to 11324 after the dry transfer process of metal electrode. The broadening of resonant peak arises from an extra optical loss from the electrode.

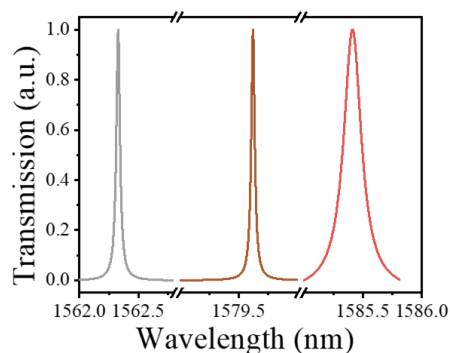


Figure S3. Variation of PCNBC's first mode resonant peak after the deposition of P(VDF-TrFE) film (Brown line), and after the metal electrode was transferred (Red line).

Appendix C Changing of transmission during the electro-optic measurements

During electro-optic measurements, the voltage is applied to the bottom electrode by attaching to the extended area of silicon waveguide, which is isolated from the Au electrode area.

In Figure 1(d), when $V_s = -20$ V, accumulation of free carriers leads to the blue-shift of resonant wavelength and strengthened light absorption, which lowers the transmission. When $0 < V_s < 10$ V, the direction of applied voltage is opposite to the direction of ferroelectric polarization. Reduction of carrier concentration weakens the light absorption, leading to the steep rise of measured transmission. When the polarization reverses, the peak current of the ferroelectric capacitor causes a sudden blue shift of the resonant wavelength and a sudden drop of transmission. Similar

process takes place during the backward sweep.

Appendix D Ferroelectric P-V loop measurement of fabricated device

Figure S4 displays the hysteresis loop of Au/P(VDF-TrFE)/Si capacitors, showing the calculated polarization as a function of applied voltage V_s . The measurement was conducted using the axiACCT TF Analyzer 3000. The operation speed of the fabricated device is tested and the results show a frequency limit of 10 kHz.

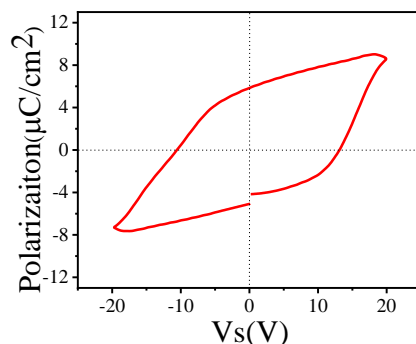


Figure S4. Measured hysteresis loop of the Au/P(VDF-TrFE)/Si capacitor.

Appendix E Performance comparison

The performance comparison between the proposed scheme in this letter and other electro-optic tuning technologies is listed in Table 1. PCNBC based electric-optic tuning with an Au/P(VDF-TrFE)/Si ferroelectric capacitor is a competitive device that well balances energy consumption and footprint.

Table 1. Benchmark table of state-of-the-art electro-optic tuning

Structure	Material	Q factor	Energy [pJ]	Footprint [μm^2]
Microring ²	Si	/	3.6 mW	260×185
Microring ³	Si	20000	0.053	78.5
Mach-Zehnder interferometer ⁴	Lithium Niobate	N/A	0.17	100×3000
Waveguide ⁵	Hf _{0.5} Zr _{0.5} O ₂	/	1.0-8.4	260 μm (length)
PCNBC (this work)	Si	20290	7.02	12

References

- 1 Quan Q, Loncar M. Deterministic design of wavelength scale, ultra-high Q photonic crystal nanobeam cavities. *Optics Express*, 2011, 19(19): 18529-42.
- 2 Cheng Z, Shu X, Ma L, et al. On-chip silicon electro-optical modulator with ultra-high extinction ratio for fiber-optic distributed acoustic sensing. *Nature Communications*, 2023, 14: 7409.
- 3 Hsu W, Nujhat N, Kupp B, et al. Sub-volt high-speed silicon MOSCAP microring modulator driven by high-mobility conductive oxide. *Nature Communications*, 2024, 15: 826.
- 4 He M, Xu M, Ren Y, et al. High-performance hybrid silicon and lithium niobate Mach–Zehnder modulators for 100 Gbit s⁻¹ and beyond. *Nature Photonics*, 2019, 13: 359–364.
- 5 Yao D, Li L, Zhang Y, et al. Energy-efficient non-volatile ferroelectric based electrostatic doping multilevel optical readout memory. *Optics Express*, 2022, 30: 13572–13582.